Journal of Orthopaedic Translation 23 (2020) 140–151

Contents lists available at ScienceDirect

Journal of Orthopaedic Translation

journal homepage: www.journals.elsevier.com/journal-of-orthopaedic-translation

Original Article

Development of a facile fluorophosphonate-functionalised titanium surface for potential orthopaedic applications

Anna I. Shiel [a], Wayne N. Ayre [b], Ashley W. Blom [c], Keith R. Hallam [d], Peter J. Heard [d], Oliver Payton [d], Loren Picco [d,e], Jason P. Mansell [a,*]

[a] Department of Applied Sciences, University of the West of England, Coldharbour Lane, Bristol, BS16 1QY, UK
[b] School of Dentistry, Cardiff University, Cardiff, CF14 4XY, UK
[c] Musculoskeletal Research Unit, University of Bristol, Southmead, Bristol, BS10 5NB, UK
[d] University of Bristol, Interface Analysis Centre, HH Wills Physics Laboratory, Tyndall Avenue, Bristol, BS8 1TL, UK
[e] Department of Physics, Virginia Commonwealth University, Richmond, 23284, VA, USA

ARTICLE INFO

Keywords:
Calcitriol
Functionalisation
Lysophosphatidic acid analogue
Osseointegration
Titanium

ABSTRACTS

Background: Aseptic loosening of total joint replacements (TJRs) continues to be the main cause of implant failures. The socioeconomic impact of surgical revisions is hugely significant; in the United Kingdom alone, it is estimated that £137 m is spent annually on revision arthroplasties. Enhancing the longevity of titanium implants will help reduce the incidence and overall cost of failed devices.

Methods: In realising the development of a superior titanium technology, we exploited the natural affinity of titanium for phosphonic acids and developed a facile means of coating the metal with (3S)1-fluoro-3-hydroxy-4-(oleoyloxy)butyl-1-phosphonate (FHBP), a phosphatase-resistant analogue of lysophosphatidic acid (LPA). Importantly LPA and selected LPA analogues like FHBP synergistically cooperate with calcitriol to promote human osteoblast formation and maturation.

Results: Herein, we provide evidence that simply immersing titanium in aqueous solutions of FHBP afforded a surface that was superior to unmodified metal at enhancing osteoblast maturation. Importantly, FHBP-functionalised titanium remained stable to 2 years of ambient storage, resisted ~35 kGy of gamma irradiation and survived implantation into a bone substitute (Sawbone™) and irrigation.

Conclusion: The facile step we have taken to modify titanium and the robustness of the final surface finish are appealing properties that are likely to attract the attention of implant manufacturers in the future.

The translational potential of this article: We have generated a functionalised titanium (Ti) surface by simply immersing Ti in aqueous solutions of a bioactive lipid. As a facile procedure it will have greater appeal to implant manufacturers compared to onerous and costly developmental processes.

Introduction

Since the 1970s, titanium and its alloys, e.g. Ti6Al4V, have found widespread application in medicine and dentistry. Examples of Ti6Al4V usage in biomedical settings include dental and orthopaedic implants, e.g. prosthetic joint replacements. The impressive strength, corrosion resistance and biocompatibility place Ti6Al4V as a choice material for implantology [1]. In spite of new approaches in the manufacture and finish of Ti6Al4V total joint replacements (TJRs) approximately 7% will fail within the lifetime of the patient. The major cause of Ti6Al4V implant failure is aseptic loosening (~80% of all revisions), which likely is a consequence of suboptimal initial osseointegration [2]. In view of the current UK's National Health Service tariffs (https://improvement.nhs.uk/resources/national-tariff/), the socioeconomic impact of aseptic loosening is significant; indeed, the cost incurred to replace failed TJRs in 2017 was approximately £137 m.

Ti6Al4V is biologically inert, which reduces the interaction of the metal with host bone tissue [3]. Encouraging host cell responses conducive to bolstering early integration into bone stems from the use of osteoconductive Ti6Al4V coatings. It is widely agreed that new Ti6Al4V technologies be developed that exhibit greater bioactivity to promote osseointegration [4], an event predicted to improve TJR longevity. One

* Corresponding author. Department of Applied Sciences, University of the West of England, Coldharbour Lane, Bristol, BS16 1QY, UK.
E-mail address: Jason.mansell@uwe.ac.uk (J.P. Mansell).

https://doi.org/10.1016/j.jot.2020.02.002
Received 2 August 2019; Received in revised form 18 December 2019; Accepted 6 February 2020
Available online 2 March 2020

way in which this could be realised is to coat the Ti6Al4V surface with agents that promote osteoblast responses synonymous with bone matrix formation and mineralisation (osteogenesis). To this end, calcium phosphates, in particular, hydroxyapatite (HAp) have been adopted as Ti6Al4V coatings because of their osteoconductive properties, which helps augment osseointegration [5]. The steps taken to coat Ti6Al4V with HAp are wide ranging and include sputter coating [6], electrophoretic deposition [7], hot isostatic pressing [8] and plasma spraying [9].

However, in spite of its enormous popularity, it is important to note that HAp will dissolve due to poor crystallised structure [10,11], which, in turn, compromises its adherence to Ti6Al4V leading to implant failure [11,12]. Low HAp coating adhesion is regarded by some to be of significant concern in the wider commercialisation of implantable devices [13–16]. Alternative solutions to HAp for improving Ti6Al4V performance have been sought and include biological coatings, e.g. parathyroid hormone. A detailed account as to the preparation of these surfaces is beyond the scope of this work, but a summary of those Ti6Al4V technologies generated over the past five years is provided (Table 1). It is noteworthy that in the majority of cases, the approaches taken towards developing these Ti6Al4V devices involve a multistep approach, sometimes requiring specialised techniques and/or noxious reagents. Clearly, there is scope to consider simpler and safer steps towards coating Ti6Al4V with osteoconductive, bioactive agents. To this end, we have focussed on lysophosphatidic acid (LPA) and selected, metabolically stabilised LPA analogues following our discovery that LPA converged with calcitriol (1,25D) in promoting human osteoblast formation and maturation [17–20]. Since osteoblast maturation is the limiting step to bone matrix calcification, agents that have the capacity to enhance this event are attractive candidates in contemporary bone biomaterial design. The LPAs are pleiotropic lysophospholipid growth factors, each composed of a fatty acyl chain, glycerol backbone and a polar phosphate head group; different LPAs vary according to acyl chain length and degree of saturation [21].

Table 1
Contemporary developments in titanium surface modification aimed at improving osseointegration.

Agent used	Modification step(s) taken	Ti type	Reference
Magnesium-substituted hydroxyapatite	Electrochemical deposition of magnesium-substituted hydroxyapatite.	Pure	[46]
Human whole blood	Titanium discs immersed in whole blood with shaking at 37 °C for 10 min.	Grade 2	[47]
Nano-hydroxyapatite loaded with rapamycin & sodium hyaluronate	Titanium steeped in a rapamycin-hyaluronate solution with ultrasonication for 12hr followed by a PBS rinse – process repeated 3 times.	TC4 alloy	[48]
Decorin-functionalised polydopamine platform	Polydopamine films deposited on titanium by exposure to aqueous dopamine hydrochloride. Resultant films capture decorin molecules.	Pure	[49]
Parathyroid hormone (PTH)	Layer-by-layer assembling technique based on the attraction between opposite charges depositing in alternate layers.	Ti6AL4V	[50]
Iron-incorporated micro/nano-hierarchical structures	Titanium samples treated with 0.1 M $FeCl_3$ for 24 h at 200 °C.	Pure	[51]
Phytic acid and $Ca(OH)_2$	Hydrothermal treatment (70 °C) of titanium using an aqueous mixture of phytic acid and $Ca(OH)_2$ for 24 h.	Grade 4	[52]
Zinc and strontium	Titanium surface modification with zinc and strontium using microarc oxidation.	Pure TA2	[53]
Calcium phosphate	Three-step soaking process; immersion in warm (37 °C) phosphate solution for 30 min, a centrifugation step followed by CaCl2 for 120 min at 80 °C.	Grade 4	[54]
Lithium chloride	Immersion of titanium in a hot (120 °C) LiOH solution (50 mM) for 12 h.	Grade 2	[55]

As phosphonic acids (PAs), the LPAs will have a natural affinity for titanium oxide (TiO_2), the natural surface finish of the metal. The interaction between PAs and TiO_2 results in the formation of stable phosphonate bonds [22,23], affording robust coatings of self-assembled layers (Fig. 1). Given the tenacity of PAs for TiO_2 and the synergistic effect of LPA and 1,25D upon osteoblast maturation, a potential candidate Ti6Al4V coating for dental and orthopaedic applications could be a potent, metabolically stabilised LPA analogue. Herein, we focus on the LPA analogue (3S)1-fluoro-3-hydroxy-4-(oleoyloxy)butyl-1-phosphonate (FHBP), which we have found works very well with active vitamin D metabolites to secure human osteoblast maturation [24–26]. In developing our FHBP-Ti6Al4V, we provide evidence for a facile coating process wherein an aqueous solution of the lipid is applied to the metal in one step under ambient conditions. Herein we provide sound evidence for the biocompatibility and stability of the coating to prolonged storage, sterilisation and physical insult.

Materials & methods

General

Unless stated otherwise, all reagents were of analytical grade and purchased from Sigma (Poole, UK).

Physiochemical characterisation of FHBP-functionalised Ti6Al4V

Magnetic sector secondary ion mass spectrometry

Secondary ion mass spectrometry (SIMS) analysis concentrated on control (blank) and 2 μM FHBP-coated specimens. The FHBP steeping concentration was informed from our previous work pertaining to the FHBP-functionalisation of HAp [27]. Two different initial surface finishes of the Ti6Al4V discs were used, as-received (presenting a relatively rough surface) and polished (smooth at the micro-scale). SIMS analysis was performed using a magnetic sector instrument comprising an FEI Company (now Thermo Fisher Scientific) (electronic variable aperture type) focused gallium ion gun fitted to a VG 7035 double-focusing magnetic sector mass spectrometer. Mass spectra, secondary ion images and depth profiles were obtained by scanning the focused gallium ion beam of 25 keV energy over the specimens and collecting the resulting secondary ions. SIMS can operate in positive and negative secondary ion mode. Surface spectra were captured in both modes, while depth profiles and ion maps were acquired mainly in negative ion mode in order to capture the fluorine, phosphate and oxygen ions, which are generally negatively charged.

Mass spectra were generally captured using a beam current of 100 pA scanned over a region of approximately 400 μm × 400 μm. For each spectrum, a mass range of 0Da–100Da was recorded, with a step size of 0.05Da and a dwell time of 100 ms per step. Under these conditions, it is estimated that during the acquisition of one spectrum, the target material would have sputtered to a depth of 0.03 nm. This is expected to be a small proportion of the coating thickness. The spectra, therefore, represent the species present at the specimen surfaces. In the SIMS measurements, it is the peak at 19Da in the negative spectra, assigned to fluorine, which is primarily indicative of the presence/absence of FHBP.

Secondary electron and secondary ion images were acquired in 640px × 480px format using a pixel dwell time of 0.2 ms–0.8 ms. The secondary

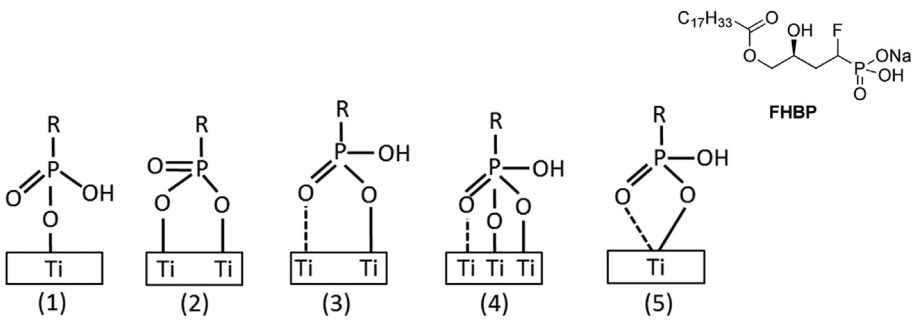

Figure 1. Overview of the predicted modes of FHBP binding at a titanium surface – (3S) 1-fluoro-3-hydroxy-4-(oleoyloxy)butyl-1-phosphonate (FHBP, sodium salt) is a phosphatase-resistant analogue of lysophosphatidic acid (LPA). As a phosphonic acid, it has a natural affinity for titanium. Depicted are the likely modes of binding; (1) monodentate, (2) and (3) bridging bidentate, (4) bridging tridentate, and (5), chelating bidentate. Phosphonic acid–titanium interactions afford robust bonding in the generation of self-assembled (mono)layers (Adapted from Ref. [22]).

ion species F^- and O^- were chosen for mapping, representing fluorine and oxygen, respectively. A secondary electron image accompanied the ion maps, showing topographical contrast.

SIMS specimens were analysed as-received and were stored between measurements under ambient laboratory conditions.

High-speed atomic force microscopy

The high-speed atomic force microscope (HS-AFM) used in this work was a custom-built, contact mode system, designed and developed in-house, permitting rapid data acquisition over large areas with sub-nanometre topological height accuracy while minimising many of the drift and noise effects that typically plague conventional AFMs [29–31]. This microscope utilised a very low spring constant silicon nitride triangle cantilever (Bruker Nano: MSNL; 0.01N/m - 0.03N/m spring constant; tip radius 2 nm nominal, 12 nm maximum). The cantilever vertical deflection was measured by a 2.5 MHz bandwidth laser Doppler vibrometer (Polytec CLV-2534) using a height decoder module. Specimens were translated in the fast (1000 Hz) and slow (1 Hz–4 Hz) scan directions by a piezo-actuated flexure stage capable of 5 μm deflection in both axes. The high-speed flexure stage was mounted on a stick-slip x-y positioner for coarse alignment (Smaract). Typically, images of size 5 μm × 5 μm, 1000px × 1000px, were captured in raster mode and rendered using customised LabView software. Each image was captured in 0.5s (two frames per second).

The original, as-received surface finish proved to be too rough for the HS-AFM technique. Therefore, analysis concentrated on imaging control (blank) and 2 μM FHBP-coated polished specimens, as informed from our previous work pertaining to the functionalisation of HAp with FHBP [27].

HS-AFM specimens were analysed as-received and stored between measurements under ambient laboratory conditions.

Surface wettability measurements

Static contact angle measurements were taken using the Model 68–76 Pocket Goniometer PGX+ and PGX+ software (Testing Machines Inc. New Castle, Delaware, USA) operated from a laptop computer. Droplets (4 μl) of cell culture-grade water were used to determine the surface wettability of control and FHBP-functionalised Ti6Al4V sample discs.

The osteoblast cell culture model

Human MG63 osteoblast-like cells (ECACC, item code: 86051601) were cultured in conventional tissue culture flasks (750 mL, Greiner, Frickenhausen, Germany) in a humidified atmosphere at 37 °C and 5% CO_2. Cells were grown to confluence in Dulbecco's modified Eagle medium (DMEM)/F12 nutrient mix (Gibco, Paisley, Scotland) supplemented with sodium pyruvate (1 mM final concentration), L-glutamine (4 mM), streptomycin (100 ng/mL), penicillin (0.1 units/mL) and 10% v/v foetal calf serum (Gibco, Paisley, Scotland). The growth media was also supplemented with 1% v/v of a 100× stock of non-essential amino acids. For experimental purposes, MG63 cells were seeded and maintained in the same growth medium but devoid of both serum and phenol red [serum-free culture medium (SFCM)].

Identified below are each of the different steps taken to develop and determine the efficacy of FHBP-Ti6Al4V to support 1,25D-induced osteoblast maturation. In some instances, Ti6Al4V dental screws were substituted for Ti6Al4V discs. For the purposes of clarity, all control and FHBP-functionalised samples were seeded with 1 ml of a 150,000 cells/ml suspension of MG63 cells in SFCM spiked with 1,25D to a final concentration of 100 nM. Cell- Ti6Al4V cultures were subsequently left for 3 days under conventional culturing conditions prior to an assessment of cellular maturation, as determined via total alkaline phosphatase (ALP) activity as detailed by us previously [20,27].

Biological optimisation of Ti6Al4V

Determining the optimal FHBP concentration

Ti6Al4V discs (10 mm × 2 mm), kindly provided by Corin (Cirencester, UK) were given a thorough distilled water rinse followed by a brief (2 min) immersion in concentrated nitric acid with gentle swirling. After thorough rinsing with distilled water, the samples were placed in aluminium foil trays and baked at 180 °C for 3 days. FHBP (LPA analogue, item code: L-9118-0.5 mg, Tebu-bio Ltd. Peterborough, UK) was reconstituted to 500 μM using 1:1 ethanol: cell culture-grade water and stored at –20 °C. For ascertaining the optimal FHBP steeping concentration for Ti6Al4V functionalisation, sample discs were placed into 24-well tissue culture plates and exposed to varying concentrations of FHBP (0.25 μM–5 μM) for a period of 24 h. Cell culture-grade water was used as the diluent. Unmodified, control Ti6Al4V discs were immersed in cell culture-grade water.

Discs were removed from the wells after 24 h and were rinsed three times in cell culture-grade water before being left to air dry within the tissue culture hood. Once dried they were transferred to a clean 24-well plate and seeded with MG63 cells. The optimal FHBP steeping concentration identified (2 μM) was used for all subsequent experiments. This test was performed in triplicate with n = 6 samples per time point with each test performed on different days and using a different passage number of cells.

Ascertaining the optimal FHBP steeping time

Cleaned and baked Ti6Al4V discs were transferred to 24-well plates. Then 1 ml of 2 μM FHBP solution was added per well and discs were steeped for a specified time period (15 min, 1 h, 2 h, 4 h or 24 h) in the solution. Control discs were steeped in the vehicle for the specified time period. The discs were removed from the wells after steeping and were rinsed three times in cell culture-grade water before being left to air dry. Once dried, they were transferred to clean 24-well plates and seeded with MG63 cells in the presence of 1,25D (100 nM). The optimal steeping time identified was used for all subsequent experiments. This experiment was performed in triplicate with n = 6 discs per time point for each test.

Determining the influence of FHBP-modified Ti6Al4V on osteoblast morphology and maturation

Ti6Al4V discs were steeped in a 2 μM solution of FHBP for 2 h. Control discs were steeped in diluent only. Modified and control discs were then rinsed three times in cell culture-grade water and left to air dry. Once dried, the discs were transferred to 24-well plates and seeded with MG63 cells using a serum-free culture medium supplemented with 1,25D to a final concentration of 100 nM.

Assessing the impact of γ-irradiation on coating efficacy

Three batches of 12 Ti6Al4V discs were steeped, on three different days, in a 2 μM solution of FHBP for 2 h. Once modified, washed and dried, half of each batch were placed in small sealable plastic bags and dispatched to Synergy Health (Swindon, UK) for γ-irradiation, as would be expected for medical device sterilisation. Sample discs received an outside dosing exposure of γ-irradiation until the dosimeter registered 35 kGy. An exposure time of 19 h was required to achieve this. The remaining Ti6Al4V samples were left stored under ambient conditions. Non-irradiated control, blank and irradiated specimens were seeded with MG63 cells. Each of the different batches was exposed to cells on different days to generate three independent experiments.

Long-term ambient storage survivorship

Ti6Al4V discs were steeped in a 2 μM solution of FHBP for 2 h. Control discs were steeped in the diluent only. Discs were either seeded with MG63 cells within 24 h of modification or stored in air for up to 2 years before conducting the cell culture experiments. Three independent experiments were performed for each of the different storage times.

Persistence of the FHBP coating to a simulated in vivo milieu

Ti6Al4V discs were steeped in 2 μM FHBP solution for 2 h. Control discs were immersed in diluent only. The discs were then individually placed within wells of a 24-well culture plate and the samples immersed in 1 ml of SFCM (see Section Physiochemical characterisation of FHBP-functionalised Ti6Al4V) and placed in a tissue culture incubator at 37 °C for 1, 3 and 7 days. After the incubation period, the SFCM was removed, spiked with 1,25D to a final concentration of 100 nM and applied to established monolayers of MG63 cells. Cells were cultured for three days prior to an assessment of their maturation via total alkaline phosphatase (ALP) assay. Each of the FHBP-Ti6Al4V discs that were steeped in SFCM were seeded with MG63 cells in the presence of 1,25D (100 nM) and left for 3 days prior to an assessment of total ALP activity.

FHBP-Ti6Al4V coating stability to Sawbone™ insertion

Ti6Al4V dental screws, kindly provided by OsteoCare (Slough, UK), were used to ascertain the effect of physical insult on FHBP coating stability. Three batches of 12 screws were steeped, on three different days, in a 2 μM aqueous FHBP solution for 2 h. Control screws were immersed in water only. Half of each batch was inserted into a mock cancellous bone substitute, Sawbone™ (item code: 1522-27 50PCF), comprising a solid, rigid, polyurethane foam. The substitute conforms to American Society for Testing and Materials (ASTM) F-1839-08 making it a 'standard material for testing orthopaedic devices and instruments'. The mechanical properties of this substitute (Table 2) place it as 'an ideal material for comparative testing of bone screws and other medical devices and instruments'. A dental drill (NSK EC BB-L) operated with a Model XP-90 power supply was used to make pilot holes in a block of the material, and the test specimens screwed in place. Once inserted, the screws were removed and cleaned under running tap water for approximately 30 s with an electrical toothbrush (ProclinicalTM C250, Colgate). Sample screws were then distilled water washed by shaking in clean universal tubes before being given three separate rinses in 70% ethanol. Samples were left to dry in a laminar flow hood before seeding with osteoblasts. A total of three independent Sawbone™ insertion experiments were performed.

Biomaterial tissue culture model

For each of the above experiments, Ti6Al4V samples were individually placed within wells of 24-well culture plates and seeded with 1 ml of a 150,000 cells/ml suspension of MG63 cells in SFCM spiked with calcitriol (1,25D, Sigma, item code: D1530-10UG) to a final concentration of 100 nM. Plates were incubated under conventional tissue culture conditions for 72 h before an assessment of osteoblast cell number and maturation.

Assessment of osteoblast number

An assessment of cell number was performed as described by us recently [27] using a combination of the tetrazolium compound 3-(4, 5-dimethylthiazol-2-yl)-5-(3-carboxymethoxy-phenyl)-2-(4-sulfophenyl)-2H-tetrazolium, inner salt (MTS, Promega, UK) and the electron-coupling reagent phenazine methosulphate (PMS). Each compound was prepared separately in pre-warmed (37 °C) phenol red-free DMEM/F12, allowed to dissolve, and then combined so that 1 ml of a 1 mg/ml solution of PMS was combined to 19 ml of a 2 mg/ml solution of MTS. A stock suspension of MG63s (1×10^6 cells/ml) was serially diluted in growth medium to give a series of known cell concentrations down to 25×10^3 cells/mL. Each sample (0.5 ml in a microcentrifuge tube) was spiked with 0.1 ml of the MTS/PMS reagent mixture and left for 45 min within a tissue culture incubator. Once incubated, the samples were centrifuged at 900 rpm to pellet the cells, and 0.1 ml of the supernatants dispensed onto a 96-well microtitre plate and the absorbances read at 492 nm using a multiplate reader. Plotting the absorbances against known cell numbers, as initially assessed through haemocytometry, enabled extrapolation of cell numbers for the experiments described herein.

Osteoblast maturation – the alkaline phosphatase (ALP) assay

An ALP substrate buffer was prepared, according to Delory and King [28]. Briefly, 0.1 M sodium carbonate and 0.1 M sodium bicarbonate solutions were blended 7:3 to achieve a pH of 10.3. The resultant solution was supplemented with $MgCl_2$ to a final concentration of 1 mM from a 1 M stock solution. A lysis solution was prepared from this buffer by performing a 10-fold dilution using cell culture-grade water followed by spiking with Triton X-100 to a final concentration of 0.1% v/v. The monolayers on the surface of the Ti6Al4V discs were lysed with 0.1 ml of this solution. After 2 min, each disc was treated with 0.2 ml of 15 mM

Table 2
Material properties of the cancellous bone substitute (Sawbone™ 1522-27 50PCF) used in this study. Each of the parameters identified are ~99% to that of human bone (https://www.sawbones.com/biomechanical/biomechanical-studies/).

Material	Density (g/cc)	Compressive strength (MPa)	Compressive modulus (MPa)	Tensile strength (MPa)	Tensile modulus (MPa)	Shear strength (MPa)	Shear modulus (MPa)
Sawbone™ 1522-27 50PCF	0.8	48	1148	27	1469	16	178

p-nitrophenylphosphate (p-NPP, di-Tris salt, Sigma, UK) prepared in the ALP buffer. Lysates were left under conventional cell culturing conditions for an hour. After the incubation period, 0.1 ml aliquots were transferred to 96-well microtitre plates, and the absorbances read at 405 nm. An ascending series of p-nitrophenol (p-NP) (50–500 μM) prepared in the substrate buffer enabled the quantification of product formation [27].

Osteoblast morphology at control and FHBP-Ti6Al4V

Cells were seeded onto control and FHBP-Ti6Al4V as per all previous experiments. After the culture period recovered samples were fixed in 2.5% paraformaldehyde in PBS for 5 min at room temperature. Once fixed, the cells were exposed to a 4′,6-Diamidino-2-phenylindole dihydrochloride (DAPI) mountant (Vector Laboratories Ltd., Peterborough, UK) to visualise nuclei and counterstained with Alexa Fluor™ 594 Phalloidin (Fisher Scientific Limited, Loughborough, UK) to detect F-actin. Cells were visualised with a Nikon Eclipse 80i (Nikon Instruments Inc., Melville, USA) fluorescence microscope with a 60 × objective and images taken using a DS-Fi1 5Mega pixel RGB camera (Nikon UK Limited, Kingston upon Thames, UK).

Statistical analysis

Results are expressed as mean ± standard deviation (SD). Statistical analyses were performed using GraphPad Prism 7.00 software. Unless otherwise stated, all data were subjected to a one-way analysis of variance (ANOVA) to test for statistical significance. A post hoc Tukey's multiple comparisons test was performed between all groups where a *p*-value of <0.05 was detected. An unpaired *t*-test (2-tailed) was used to compare means of modified and unmodified discs and of freshly used and

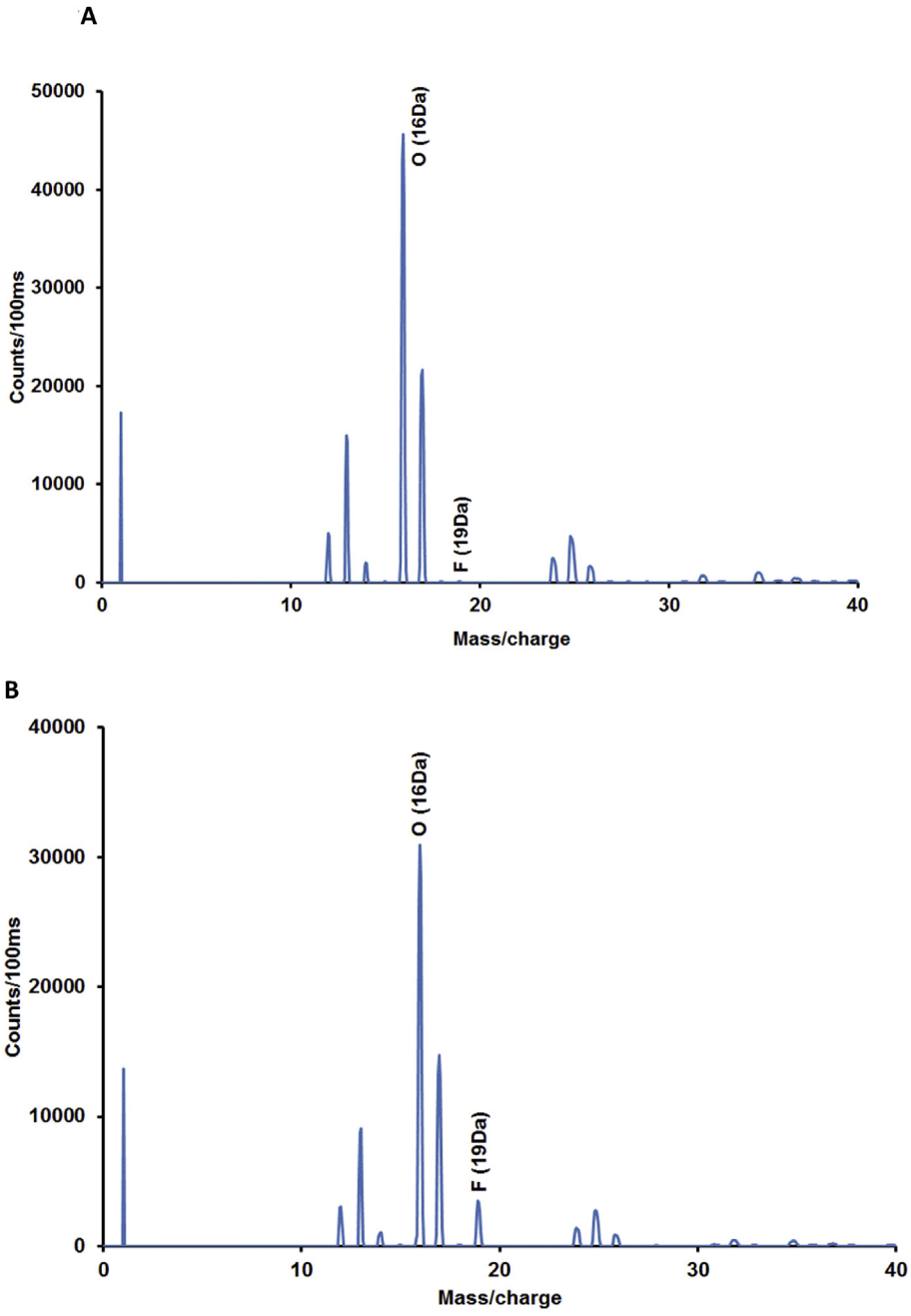

Figure 2. Negative ion SIMS spectra of fresh, polished Ti6Al4V specimen surfaces: A) Control (blank); B) 2 μM FHBP-coated – Small discs of freshly polished and coated Ti6Al4V material were analysed by secondary ion mass spectrometry, using a focused gallium ion beam as the primary ion source. Emitted secondary ions were collected and mass-analysed to produce the spectra shown above. Peaks with mass/charge ratios of 1, 12, 13, 14, 16, 17, 19, 24, 25 and 26 arise from negatively-charged secondary ions H, C, CH, CH_2, O, OH, F, C_2, C_2H and CN, respectively. SIMS is very surface sensitive, with the depth of analysis being only 1–2 atom layers. The fluorine peak at mass/charge = 19 in the lower figure is indicative of the FHBP coating adhering to the surface of the sample. An indication of FHBP coverage is calculated from the ratio of the F^- (mass 19) to the O^- (mass 16) peaks, to account for variations in instrument sensitivity.

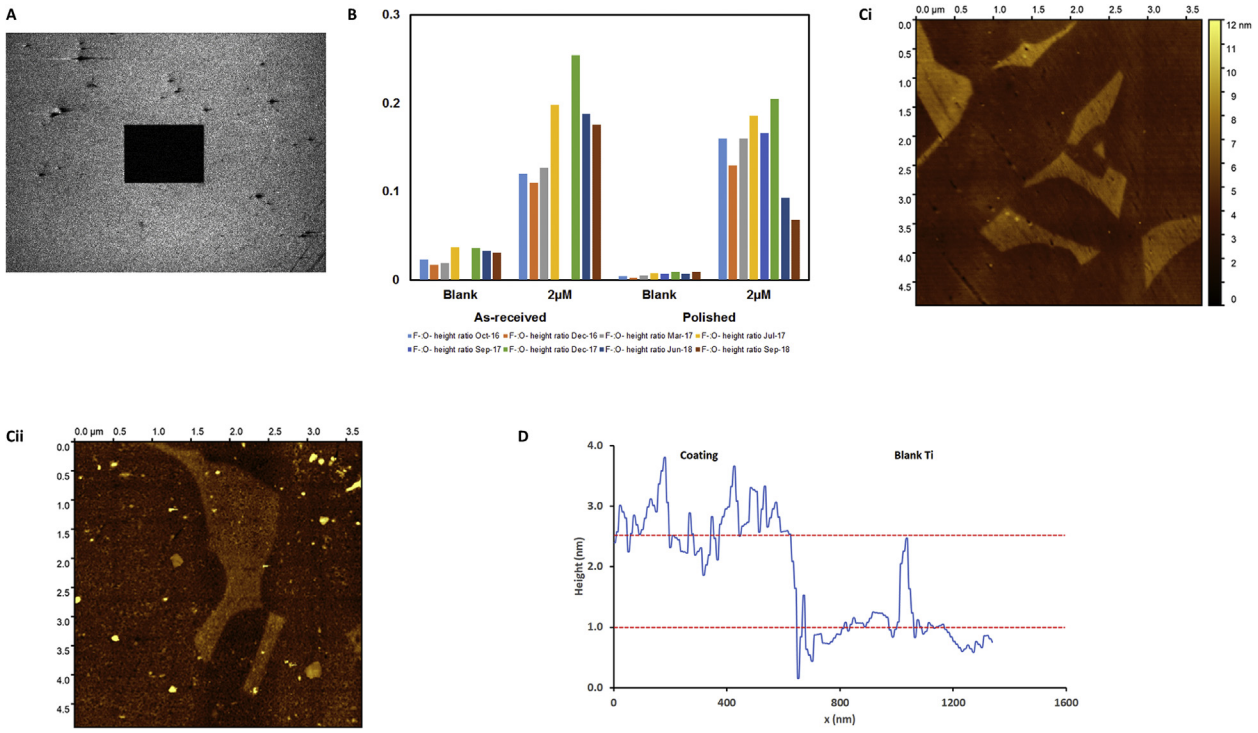

Figure 3. Surface topography of FHBP-Ti6Al4V – **A.** Negative ion fluorine peak (mass/charge = 19) SIMS map of 2 μM FHBP-coated, fresh, polished Ti6Al4V, demonstrating that, apart from surface debris, fluorine (representative of FHBP) evenly covers the surface. The central black rectangle shows where a depth profile was performed, etching away the fluorine-containing species. The image field width is ~400 μm. **B.** SIMS fluorine to oxygen (mass/charge = 16) peak height ratios for as-received and polished Ti6AL4V, blank and 2 μM FHBP-coated, as a function of measurement date - The two blank (untreated) samples show low values, though non-zero in the as-received material due to some fluorine contamination. 2 μM FHBP-treated Ti6AL4V shows high values, indicating the continuing presence of FHBP over two years. **C.** HS-AFM height maps of fresh, polished Ti6Al4V: **i**) Control (blank); **ii**) 2 μM FHBP-coated - The larger polygonal shapes are a harder phase of the Ti6AlV left proud of the surrounding material due to polishing rate differences. The smaller high features are likely contaminants and residue from the polishing and FHBP coating steps. **D.** HS-AFM measurement of 2 μM FHBP coating thickness - Line profile across a transition from coating to bare Ti6AlV surface created by mechanical scraping, showing the film to be ~1.5 nm thick.

stored modified discs. *p*-values of <0.05 were considered statistically significant.

Results

Magnetic sector secondary ion mass spectrometry

Positive and negative SIMS spectra, depth profiles and maps were obtained from as-received and polished Ti6Al4V specimens that were either untreated or had been treated with aqueous 2 μM FHBP. Negative ion spectra, via their ratios of the peak heights for fluorine (19Da) and oxygen (16Da), confirm the presence of FHBP on the surfaces of coated specimens (Fig. 2). A negative ion SIMS map of fluorine for 2 μM-coated polished specimens demonstrates that the FHBP is evenly distributed across the surface (Fig. 3A). We also monitored coating stability, looking to see if there were any signs of reduction of the amount of surface coating. The ratios of the peak heights for fluorine (19Da) and oxygen (16Da), for as-received and polished specimens, and as a function of the measurement date, are shown graphically (Fig. 3B). This ratio was taken to correct for any changes in absolute signal strength from specimen to specimen. Similar information can be obtained by looking at maps of the distribution of these elements across the sample surface. We have been able to analyse the same areas on the same specimens over a period of almost two years. In the vast majority of cases, both spectra and maps have remained consistent throughout the duration of the project, indicative of the continuing presence of the active coating on the specimen surfaces.

High-speed atomic force microscopy (HS-AFM)

The HS-AFM micrographs (Fig. 3C) represent the fresh control (blank) and 2 μM FHBP-coated specimens. In both cases, the major contrast differences seen are due to surface height differences in the polished discs, in turn, attributed to different hardnesses present within the two-phase Ti6Al4V alloy material. However, in addition, the presence of the surface coating was clearly evident in images of the 2 μM FHBP specimen. The coating was found to be ubiquitous across the sample surface and very durable. Attempts to scratch through with the AFM cantilever failed. However, the layer did seem to consist of a porous structure rather than a homogeneous coating. Scaling these images to the same height range and recording line profile across the specimens revealed the coating to increase the roughness of the surface noticeably (Ra (uncoated) = 0.834 nm; Ra (coated) = 0.910 nm). When imaging the 2 μM FHBP-coated specimen two months later, the coating was found to be more fragile and more easily damaged by excessive tip-imaging forces. This did, though, allow us, by using the HS-AFM probe tip, to scrape away the surface film and create a measurable step height change. By these means, it was then possible to show the film to be up to ~1.5 nm thick (Fig. 3D). HS-AFM images obtained from the same areas (for the best comparison of surfaces with time) on blank and 2 μM FHBP-coated polished Ti6Al4V specimens have largely shown no obvious signs of changes in the active film with storage time. After many months of storage, there were signs that gaps had started to appear in the coating, revealing the underlying Ti beneath. Later images appeared to show the film to have degraded somewhat. However, immediately-adjacent areas of the film retained appearances akin to that of the original area when first imaged.

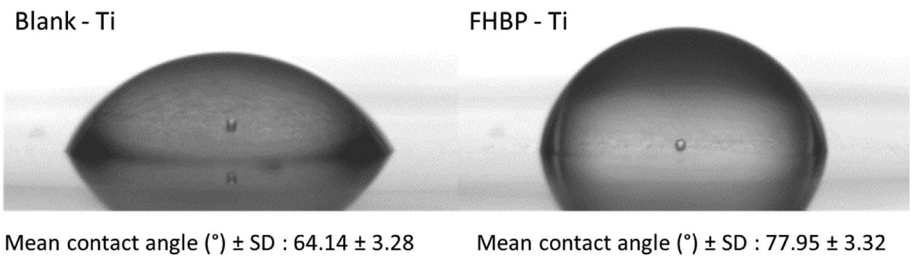

Figure 4. Contact angle measurements for bare and FHBP-functionalised Ti6AL4V – Six clean Ti6AL4V (Ti) discs (Blank-Ti) were randomly selected from a batch of samples and six contact angle measurements taken for each disc (64.14 ± 3.28°). All discs were then steeped in a 2 μM aqueous solution of FHBP for 2 h, retrieved, rinsed twice with distilled water, and then allowed to dry in a laminar flow cabinet. Once dried six contact angle measurements were taken again for each of the sample discs (FHBP–Ti). FHBP-functionalisation resulted in a modest and significant increase ($*p < 0.001$) in the contact angle by approximately 21% (77.95 ± 3.32°).

Therefore, it is believed that the observed degradation was most likely a consequence of repeated imaging rather than the effect of storage under ambient conditions.

Coating Ti6Al4V with FHBP modestly increases surface hydrophobicity

Titanium discs (n = 6) were randomly selected from a batch of samples and six contact angle measurements taken for each disc (64.14 ± 3.28°). All discs were then steeped in a 2 μM aqueous solution of FHBP for 2 h, retrieved, rinsed twice with distilled water and allowed to dry. Once dried, six contact angle measurements were taken again for each of the sample discs. FHBP-functionalisation resulted in a modest and significant increase ($*p < 0.001$) in the contact angle by approximately 21% (77.95 ± 3.32°). Images taken for the water droplets at the control and functionalised Ti6Al4V (Fig. 4) give a clear indication for a change in surface wettability.

FHBP-functionalisation of Ti6Al4V produces a biologically active surface finish

Informed from our previous work using HAp [27], we conducted a pilot experiment wherein Ti6Al4V discs were exposed to aqueous FHBP (0.5 – 2 μM) for a period of 24 h. Each of these different treatments produced a functionalised surface that supported 1,25D-induced MG63 maturation, as determined via total ALP activity (Fig. 5A). Compared to control metal, each of the FHBP-functionalised samples significantly improved the maturation response by approximately 5 fold ($p < 0.001$). Whilst the data indicate a modest improvement in the osteoblast response at 2 μM FHBP-Ti6Al4V compared to 0.5 μM FHBP-Ti6Al4V, the data did not reach statistical significance.

In the second set of pilot experiments, we examined the speed with which FHBP could produce a functionalised Ti6Al4V surface capable of enhancing 1,25D-induced osteoblast maturation. In light of the data presented in Fig. 5A, we selected 2 μM FHBP as the steeping concentration for Ti6Al4V. The data presented support a good maturation response of osteoblasts at Ti6Al4V surfaces exposed to FHBP for as little as 15 min (Fig. 5B). Increasing the steeping time to 2 h culminated in a further significant increase ($p < 0.0001$) in MG63 maturation compared to control Ti6Al4V ($p < 0.0001$). An FHBP exposure time of 2 h appeared optimal, and this was selected for the remaining experiments. An assessment of MG63 morphology at the control and FHBP-Ti6Al4V (Fig. 6) supported the expected change in cell shape consequent to LPA receptor-mediated alterations in cytoskeletal dynamics. Cells at FHBP-Ti6Al4V were slightly larger, and the signal intensity for F-actin was noticeably more intense.

FHBP-Ti6Al4V is stable to prolonged ambient storage

Orthopaedic and dental Ti6Al4V devices are stored packaged, in air, under ambient conditions, often for many months prior to implantation. We, therefore, examined the efficacy of FHBP-Ti6Al4V to enhance 1,25D-induced osteoblast maturation following prolonged ambient storage. The data presented (Fig. 7) clearly indicate that compared to control metal, FHBP-Ti6Al4V continues to bolster MG63 maturation even after 2 years of storage ($p < 0.0001$).

FHBP-functionalised Ti6Al4V withstands γ-irradiation, insertion into Sawbone™ and exposure to a simulated in vivo milieu

Medical implants are invariably sterilised using γ-irradiation. Typical outside dosing can be in the range of 25–35 kGy for joint prostheses. FHBP-functionalised Ti6Al4V was examined for its ability to support 1,25D-induced osteoblast maturation following 35 kGy outside dosing (Fig. 8A). As anticipated, non-irradiated functionalised surfaces supported a good maturation response compared to bare metal ($p < 0.0001$). Similarly irradiated FHBP-Ti6Al4V secured a clear maturation response of MG63 cells compared to non-functionalised controls ($p < 0.0001$). However, over the three independent experiments, we consistently found a modest, yet statistically significant reduction ($p < 0.001$), in the ability of irradiated samples to support 1,25D-induced cellular maturation compared to non-irradiated functionalised controls. On average, this decline in potency was approximately 25%.

Next, we examined the robustness of the FHBP coating to withstand the rigours of insertion into a solid block of Sawbone™. For these particular tests, dental screws fashioned from the same Ti6Al4V alloy were used. The evidence presented (Fig. 8B) indicates that FHBP-functionalised Ti6Al4V screws retain bioactivity after mock bone implantation, retrieval and washing. Importantly the ability of implanted and non-inserted functionalised controls to enhance 1,25D-induced MG63 maturation was similar. Collectively the findings presented indicate an FHBP coating that demonstrates good survivorship to physical insult.

In a final set of experiments, we examined if the FHBP coating was retained on the Ti6Al4V surface following a 1 week exposure to SFCM at 37 °C. When MG63 cells were seeded onto these SFCM-treated discs, the extent of maturation, as determined via total ALP activity, was comparable to cells at untreated FHBP-Ti6Al4V surfaces (Fig. 9A). The recovered, conditioned, SFCM (CM) was spiked with 1,25D to a final concentration of 100 nM and applied to established monolayers of cells. From the data provided (Fig. 9B), it would appear that little/no FHBP had leached from the functionalised Ti6Al4V as the extent of cellular maturation was comparable to cells treated with FHBP (250 nM) alone.

Discussion

Aseptic loosening of TJRs is expected to increase given the prediction of a rise in the elderly demographic. Reducing the socioeconomic impact of revision arthroplasties for these implant failures is, therefore, an ongoing area of active research and development. Improving the longevity of TJR technologies could include simple biological coatings aimed at encouraging early, enhanced osseointegration. Simple solutions that deliver on these properties are more likely to be adopted by the implant manufacturers compared to more complex, costly and time-consuming strategies.

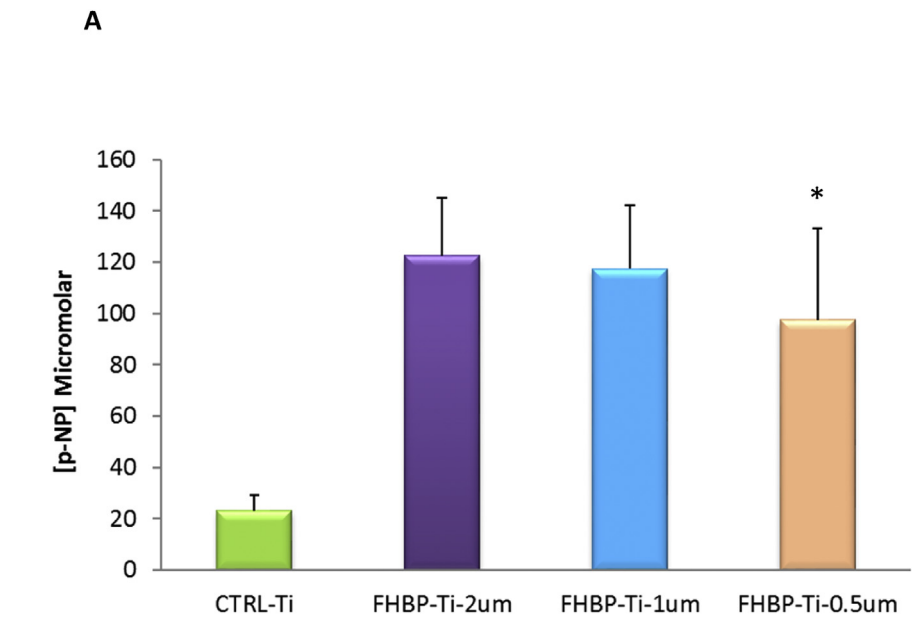

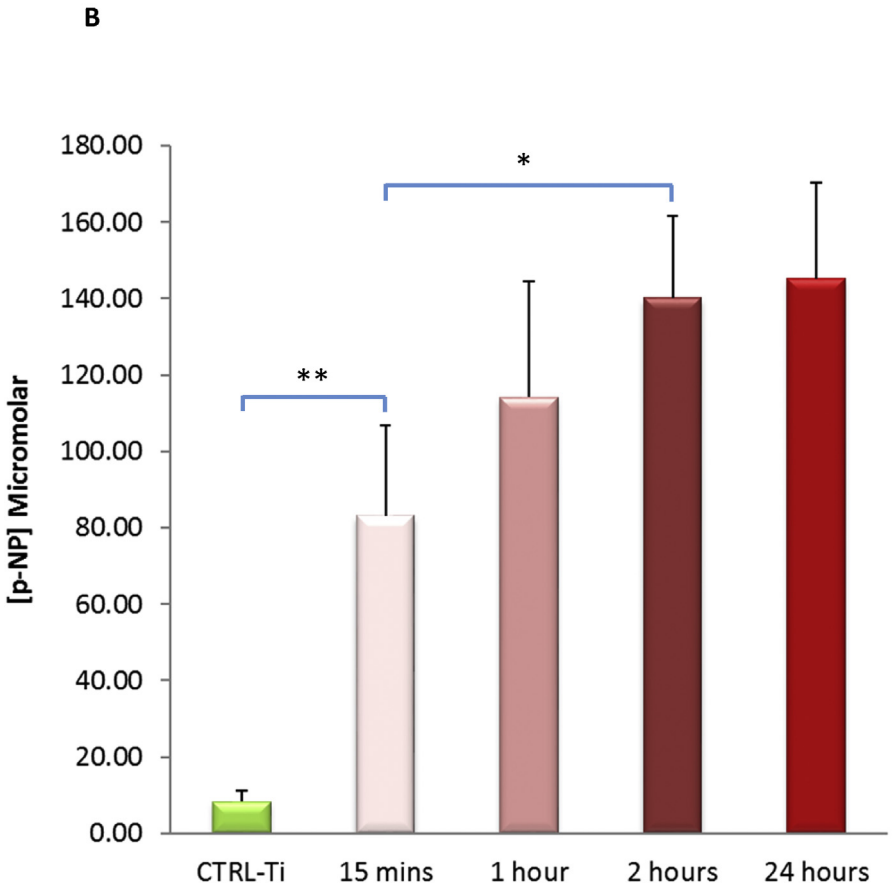

Figure 5. Direct functionalisation of Ti6AL4V with FHBP supports 1,25D-induced osteoblast maturation – **A.** Orthopaedic-grade Ti6AL4V (Ti) discs (12 mm diameter, 1 mm thick) were individually housed in multiwell plates and steeped in aqueous solutions of FHBP (0.5 – 2 μM) for 24 h. After rinsing and drying, all discs were seeded with MG63 osteoblasts at a density of 15×10^4 cells/ml/disc in the presence of 100 nM 1,25D. After a 3-day culture, an assessment of MG63 maturation was determined via a total alkaline phosphatase (ALP) assay. Greater concentrations of p-nitrophenol (p-NP) generated from the hydrolysis of p-nitrophenyl phosphate are indicative of raised ALP activity, a feature of mature osteoblasts. Depicted are the pooled data from three independent experiments. Each bar (N = 18) represents the mean micromolar concentration of p-NP plus the standard deviation. An FHBP steeping concentration as low as 500 nM generated Ti6AL4V surfaces that were superior to control (CTRL)-Ti (*$p < 0.001$) at supporting 1,25D-induced MG63 maturation. **B.** An FHBP (2 μM) steeping time of only 15 min generated Ti6AL4V surfaces that were superior to CTRL-Ti (**$p < 0.001$) at supporting 1,25D-induced MG63 maturation. By increasing the steeping time for a further 105 min added a significant (*$p = 0.001$) improvement in the maturation response. The data depicted are represented from two independent experiments and are expressed as the mean micromolar concentration of p-NP plus the standard deviation. For each bar N = 6.

Coating Ti6Al4V with biologicals that are clearly connected to osteoblast formation and maturation is certainly nothing new. Indeed osteoinductive bone morphogenic proteins (BMPs), for example, have been considered attractive candidates for bone biomaterial functionalisation for approximately two decades [32,33]. However, getting those molecules securely fastened in a functional, reversibly bound form is especially challenging, particularly if they are large protein growth factors; rigid linkages between the protein and the material surface can lead to loss of function consequent to tertiary structure collapse [34]. In addition, many of the steps taken to secure these factors at the metal

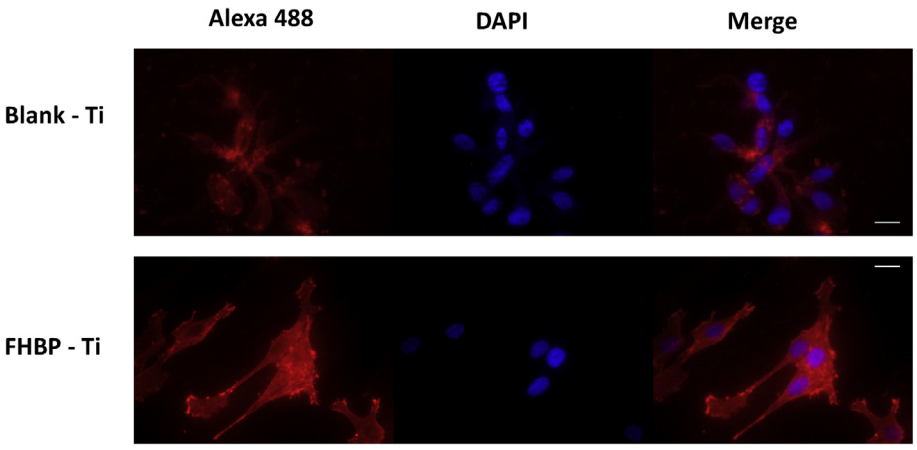

Figure 6. MG63 cell morphology at FHBP-functionalised Ti6AL4V – Cells were seeded onto control (Blank-Ti) and FHBP-functionalised Ti6AL4V (FHBP–Ti) and cultured, under conventional conditions for 3 days. Once cultured, the sample discs were recovered, fixed in paraformaldehyde and the cells stained to visualise nuclei (DAPI) and F-actin (Alexa 488). In keeping with the reported effects of LPA (FHBP) on the cytoskeleton, it is clear that MG63 cells are slightly larger at FHBP-Ti surfaces and exhibit more intense staining for F-actin. Scale bar: 20 μM.

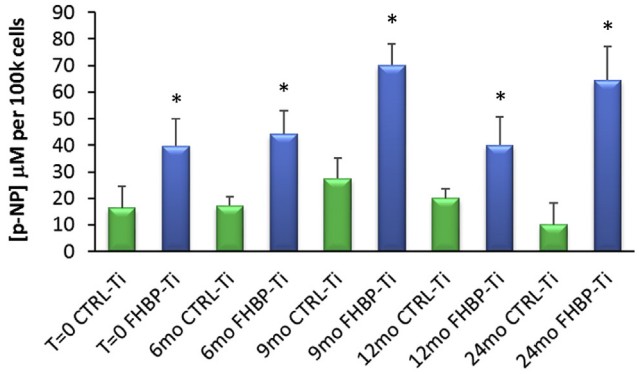

Figure 7. FHBP-functionalised Ti6AL4V is stable to prolonged ambient storage in air – A total of 30 orthopaedic-grade Ti6AL4V (Ti) discs (12 mm diameter, 1 mm thick) were individually housed in multiwell plates and steeped in a 2 μM aqueous solution of FHBP for 2 h. Thirty control sample discs (CTRL-Ti) were immersed in distilled water only for the same time. Within 48 h of treatment (T = 0) control and functionalised discs were seeded with MG63 osteoblasts at a density of 15×10^4 cells/ml/disc in the presence of 100 nM 1,25D. All other discs were transferred to sterile 24-well plates and stored under ambient conditions in the air. At the desired time points, (6–24 months), control and functionalised specimens were seeded with MG63 cells, as indicated above. In each instance, the cells were cultured for 3-days under conventional conditions, after which the discs were transferred to clean plates to assess osteoblast maturation via a total alkaline phosphatase (ALP) assay. The data depicted for T = 0, 12 and 24 months are the pooled data from three independent experiments. For each bar N = 18. Data for T = 6 and 9 months are the pooled data from two independent experiments. For each bar N = 12. All data are expressed as the mean micromolar concentration of p-NP plus the standard deviation. From the findings presented, it is clear that at each time point, FHBP-Ti is better than control metal at supporting osteoblast maturation (*$p < 0.001$).

surface require coupling molecules, e.g. silanes (e.g. Ref. [35]) and/or onerous, multistep operating conditions employing highly noxious reagents, e.g. Piranha solution (e.g. Ref. [36]). In the context of BMP-2-functionalised Ti6Al4V, Kashigawi and colleagues [33] modified this growth factor with a peptide motif (RKLPDA) known to bond electrostatically to Ti6Al4V [37,38]. Such an approach comes at significantly added cost to existing Ti6Al4V technologies, and to date, this novel, innovative approach to improving Ti6Al4V prosthesis longevity has not been adopted by any of the implant manufacturers.

Given some of the limitations that polypeptide/protein growth factors have as Ti6Al4V coatings, e.g. susceptibility to proteases, supra-physiological concentrations and/or possible immunogenic reactions, it would be advantageous to utilise much smaller molecules. If these molecules, in turn, could be applied to Ti6Al4V (or indeed HAp) without the need for bespoke linkers and/or technically challenging procedures, then they start to become far more appealing to the implant manufacturers. The simplest growth factor known to target human osteoblasts and bone marrow-derived stem cells is LPA [39]. Of particular significance to bone health is our discovery that LPA, and certain LPA analogues, converge with 1,25D to enhance human osteoblast formation and maturation [17,19,20,24,25,40]. Fortuitously the LPAs are phosphonic acids, bearing polar phospho-head groups, which have a natural affinity for TiO_2, the natural surface finish of the metal [22,23]. Their interaction with Ti6Al4V affords the provision of securely fastened self-assembled layers that are still able to signal transduce when osteoblasts arrive at the functionalised surface [26].

Herein we present good evidence for the facile, direct modification of Ti6Al4V with FHBP, a potent, phosphatase-resistant analogue of LPA. In our experiments, we found that Ti6Al4V could be functionalised with FHBP within 15 min using water as the solvent at room temperature. Increasing the steeping time to 2 h afforded significant improvements in surface functionality. Evidence of FHBP-Ti6Al4V functionality was based on the ability of this surface to enhance 1,25D-induced osteoblast (MG63) maturation, as supported by elevated total alkaline phosphatase (ALP) activity. The enzyme is inextricably linked to bone matrix calcification [41], and therefore, overall osteogenesis, forming an essential aspect of bone biomaterial osseointegration. Biomaterial modifications that induce significant increases in human osteoblast ALP are, therefore, a very positive feature. The physiochemical evidence provided in this report support the expected outcome for the interaction of TiO_2 with FHBP, as based on the known modes of phosphonic acid-binding to this metal oxide [22]. From the SIMS and HS-AFM analysis results it is evident, that for both 'as-received' and polished Ti6Al4V surfaces, that the FHBP coating has remained present in significant quantities after storage for at least two years under ambient conditions. We also found that exposing FHBP to Ti6Al4V modestly reduced surface wettability ($77.95 \pm 3.32^\circ$) by approximately 21% compared with unmodified Ti6Al4V ($64.14 \pm 3.28^\circ$). This increase in the contact angle would be expected for a Ti6Al4V surface coated with a lysophospholipid bearing an oleoyl acyl chain.

In taking our first steps to realising the potential of FHBP-Ti6Al4V for orthopaedic/dental applications, it is imperative that an assessment of biomaterial stability be ascertained. To this end, we have focussed on FHBP-coating stability to long-term (2 years) ambient storage, survivorship to γ-irradiation and persistence of the Ti6Al4V coating following insertion into a mock bone substitute, Sawbone™. With regard the latter, this approach has been informed by our studies using juvenile porcine mandibles and FHBP-functionalised dental screws [42]. We quickly learned that the abundant ALP in the bone tissue rapidly adsorbed (within minutes) to implanted Ti6Al4V screws. Since ALP is the endpoint we had to source an alternative material to native bone tissue to bypass

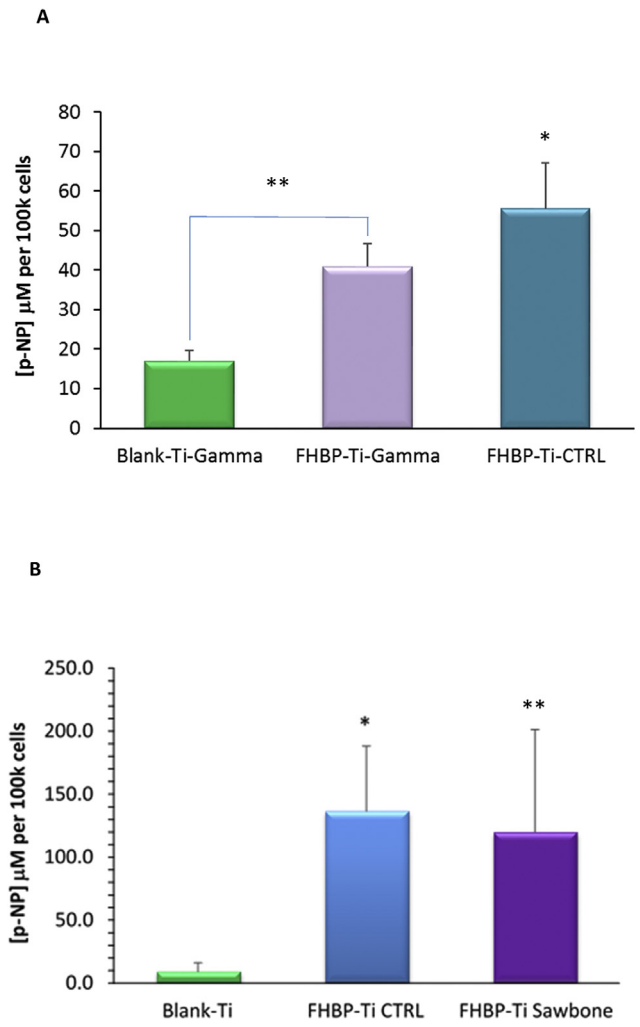

Figure 8. FHBP-coating survivorship at Ti6AL4V following γ-irradiation and insertion into a cancellous bone substitute – **A.** On three independent occasions twelve orthopaedic-grade Ti6AL4V (Ti) discs (12 mm diameter, 1 mm thick) were individually housed in multiwell plates and steeped in a 2 μM aqueous solution of FHBP for 2 h. A dozen blank sample discs (Blank-Ti-Gamma) were immersed in distilled water only for the same time. For each batch of blank and functionalised specimens, half were stored under ambient conditions in air. The remaining discs were dispatched for outside γ-irradiation dosing at ~35 kGy. Each batch of sample discs was seeded, on three separate days, with MG63 osteoblasts at a density of 15×10^4 cells/ml/disc in the presence of 100 nM 1,25D. After a 3-day culture, the discs were transferred to clean plates to assess osteoblast maturation via a total alkaline phosphatase (ALP) assay. The data depicted are the pooled data from three independent experiments and are expressed as the mean micromolar concentration of p-NP per 100 k cells, plus the standard deviation. For each bar N = 18. As anticipated, non-irradiated FHBP-Ti controls (FHBP–Ti-CTRL) were superior to blank discs in supporting 1,25D-induced cellular maturation. FHBP-functionalised discs that had been irradiated (FHBP–Ti-Gamma) were also better than blanks in promoting 1,25D-induced differentiation (**$p < 0.0001$) but they were significantly (*$p < 0.001$) less potent than the FHBP-Ti-CTRL group. **B.** On three separate occasions, twelve Ti6AL4V (Ti) dental screws (OseoCare, Slough, UK) were immersed in 2 μM aqueous FHBP for 2 h. Of these, half were implanted into a solid block of mock bone (Sawbone™) using a dental drill. Once implanted, the screws were retrieved, washed under running tap water to remove trapped particles and subsequently prepared for osteoblast cell culture. As anticipated, non-inserted functionalised samples (FHBP–Ti-CTRL) supported significantly greater 1,25D-induced cell maturation (*$p < 0.001$) compared to unmodified dental screws (Blank-Ti). Similarly, mock bone-inserted modified specimens (FHBP–Ti Sawbone™) supported greater MG63 maturation compared to blank-Ti (**$p <$ 0.001). The similar extent of cellular maturation for both sets of functionalised screws is evidence of coating survivorship to the rigours of implantation.

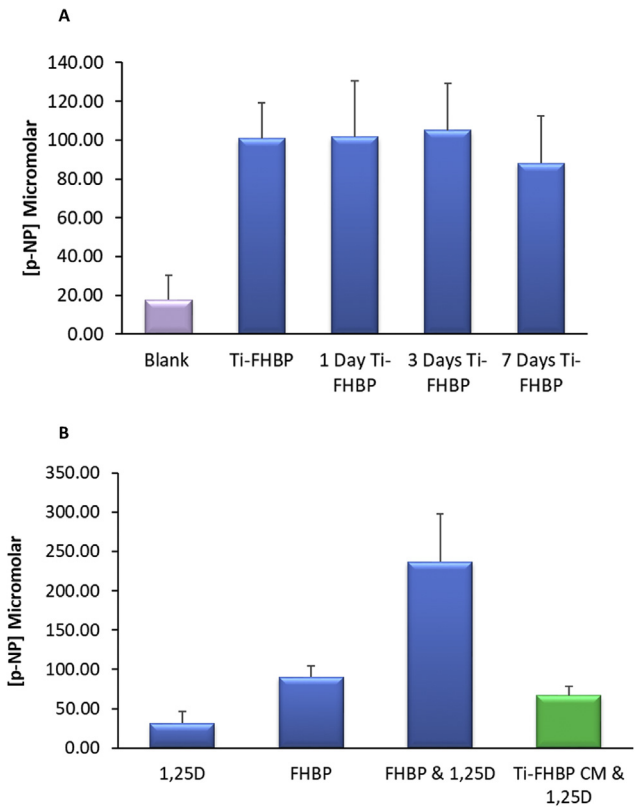

Figure 9. Evidence for the persistence of FHBP at a Ti6AL4V (Ti) surface after a 7 day exposure to a simulated *in vivo* milieu – **A.** Ti6AL4V (Ti) discs were functionalised with aqueous FHBP (2 μM) and either left 'as is' (Ti-FHBP) or steeped in a serum-free cell culture medium (SFCM) for up to 1 week at 37 °C. At each of the indicated times, sample discs were recovered, rinsed, and seeded with MG63 cells in the presence of 100 nM 1,25D and an assessment of total ALP activity determined following a 72hr culture. The findings presented indicate that each of the SFCM-treated Ti6AL4V samples exhibits comparable (ALP) activity to the control, 'as is', Ti-FHBP. **B.** The conditioned SFCM (CM) recovered from Ti-FHBP following a 7 day SFCM exposure were spiked with 1,25D to a final concentration of 100 nM and applied to established monolayers of MG63 cells. Cultures were maintained for three days prior to total ALP activity assays. As anticipated, the co-treatment of MG63 cells with 1,25D (100 nM) and FHBP (250 nM) led to a clear increase in total ALP activity, as supported by the greater concentration of p-nitrophenol (p-NP) generated from p-nitrophenyl phosphate. In contrast, the 1,25D-supplemented CM was associated with a low total ALP activity. Each data set is the pooled mean results from three independent experiments (n = 18), performed on different days, + the SD.

the unavoidable contamination of our functionalised Ti6Al4V with this enzyme. We, therefore, chose a cancellous bone surrogate (Sawbone™) with material properties close to those of natural tissue (Table 2).

The findings presented in this report for Sawbone™-implanted Ti6Al4V dental screws are encouraging as anticipated from our previous work [42]; FHBP-Ti6Al4V dental screws supported a good maturation response of osteoblasts to 1,25D. The extent of cellular maturation was similar to FHBP-Ti6Al4V screws inserted into the cancellous bone substitute. In addition to these samples being inserted into Sawbone™, retrieved screws were cleaned with an electric toothbrush under running tap water. Collectively these findings indicate a robust coverage of FHBP at the Ti6Al4V surface that has the potential to survive the rigours of actual arthroplasty.

Total joint prostheses and Ti6Al4V dental implants are packaged for ambient storage in air. Depending on the type of device and the age of the recipient, some of these implants can remain stored for many months, sometimes years. Whatever the biological coating type, it must be able to withstand conventional storage for prolonged periods. We, therefore,

examined the biological performance of our FHBP-Ti6Al4V over a two-year period. When osteoblasts were seeded onto these stored samples, they were consistently superior to control, unmodified Ti6Al4V, at enhancing 1,25D-induced cellular maturation. The extent to which the cells differentiated after a two-year storage period was similar to freshly functionalised Ti6Al4V. These are very encouraging findings, and we are continuing to ascertain FHBP stability at Ti6Al4V for a further 3 years of ambient storage.

Prior to their dispatch to the health services, packaged prostheses are subjected to γ-irradiation to guarantee their sterilisation. Therefore, during the course of our study, we subjected FHBP-functionalised Ti6Al4V to 35 kGy outside dosing of γ-irradiation. Herein we provide evidence that γ-irradiated FHBP-Ti6Al4V was better than control metal at supporting 1,25D-induced cellular maturation. However, in contrast to non-irradiated functionalised controls, γ-irradiation does impact negatively on the biological activity of the adsorbed lipid. The extent of reduced FHBP potency was fairly consistent and statistically significant for each of the three independent experiments by approximately 25%. The finding that the majority of the FHBP activity persisted soon (within 1 week) after ionising radiation is certainly encouraging. We also found, from a single experiment, that irradiated FHBP-Ti6Al4V retained comparable activity to freshly irradiated samples even after 18 months of ambient storage, suggesting little/no post-irradiation compromise to the FHBP coating (data not shown).

Conclusion

During the course of our study, we found no reports detailing the long-term stability and/or survivorship of any biological coating at a titanium surface. This is particularly surprising given the constraints around medical device storage and use. To summarise, we have developed a biologically functionalised titanium surface finish that appears to be stable to at least two years of ambient storage. The finding that the Ti6Al4V -bound FHBP could withstand insertion into a mock bone substitute, resist irrigation and withstand γ-irradiation are important outcomes in overall product development. The approach we have taken to biologically functionalise titanium is very simple; a facile, dip coating approach for (bio)material modifications is particularly attractive since there is no requirement for specialist equipment, and the coating process is not constrained to a specific feature [43–45]. These are important considerations in realising the fabrication of new implantable Ti6Al4V technologies which could now extend to bioactive phosphatase-resistant LPA analogue coatings.

Author contributions

JPM designed the project and wrote the manuscript. All cell culture studies were conducted by AIS whilst KRH, PJH, OP and LP performed the physiochemical analyses detailed in this work. All authors participated in the review and discussion of the manuscript.

Conflict of Interest

The authors have no conflicts of interest to disclose in relation to this article.

Acknowledgements

This study is funded by the National Institute for Health Research (NIHR) [Invention for Innovation (II-LA-0315-20004)]. The views expressed are those of the author(s) and not necessarily those of the NIHR or the Department of Health and Social Care.

We are especially grateful to Corin (Cirencester, UK) and OsteoCare (Slough, UK) for the very generous supply of the titanium materials used in the study.

References

[1] Sidambe AT. Biocompatibility of advanced manufactured titanium implants—a review. Materials 2014;7:8168–88.
[2] National joint registry (England, Wales, Northern Ireland and the Isle of Man), 15th annual report. 2018.
[3] Vanderleyden E, Van Bael S, Chai YC, Kruth JP, Schrooten J, Dubruel P. Gelatin functionalised porous titanium alloy implants for orthopaedic applications. Mater Sci Eng C 2014;42:396–404.
[4] Apostu D, Lucaciu O, Lucaciu GDO, Crisan B, Crisan L, Baciut M, et al. Systemic drugs that influence titanium implant osseointegration. Drug Metab Rev 2017;49:92–104.
[5] Spriano S, Yamaguchi S, Baino F, Ferraris SA. Critical review of multifunctional titanium surfaces: new frontiers for improving osseointegration and host response, avoiding bacteria contamination. Acta Biomater 2018;79:1–22.
[6] Ding S-J. Properties and immersion behaviour of magnetron-sputtered multi-layered hydroxyapatite/titanium composite coatings. Biomaterials 2003;24:4233–8.
[7] Han Y, Fu T, Lu J, Xu K. Characterization and stability of hydroxyapatite coatings prepared by an electrodeposition and alkaline-treatment process. J Biomed Mater Res 2000;54:96–101.
[8] Wie H, Herø H, Solheim T. Hot isostatic pressing-processed hydroxyapatite-coated titanium implants: light microscopic and scanning electron microscopy investigations. Int J Oral Maxillofac Implants 1998;13:837.
[9] De Groot K, Geesink R, Klein C, Serekian P. Plasma sprayed coatings of hydroxylapatite. J Biomed Mater Res 2004;21:1375–81.
[10] Tong W, Yang Z, Zhang X, Yang A, Feng J, Cao Y, et al. Studies on diffusion maximum in x-ray diffraction patterns of plasma-sprayed hydroxyapatite coatings. J Biomed Mater Res 1998;40:407–13.
[11] Garcia F, Arias J, Mayor B, Pou J, Rehman I, Knowles J, et al. Effect of heat treatment on pulsed laser deposited amorphous calcium phosphate coatings. J Biomed Mater Res 1998;43:69–76.
[12] Watson C, Tinsley D, Ogden A, Russell J, Mulay S, Davison E. Implants: a 3 to 4 year study of single tooth hydroxylapatite coated endosseous dental implants. Br Dent J 1999;187:90–4.
[13] Mohseni E, Zalnezhad E, Bushroa AR. Comparative investigation on the adhesion of hydroxyapatite coating on Ti–6Al–4V implant: areview paper. Int J Adhesion Adhes 2014;48:238–57.
[14] Wang RR, Welsch GE, Monteiro O. Silicon nitride coating on titanium to enable titanium–ceramic bonding. J Biomed Mater Res 1999;46:262–70.
[15] Sun L, Berndt CC, Gross KA, Kucuk A. Material fundamentals and clinical performance of plasma-sprayed hydroxyapatite coatings: a review. J Biomed Mater Res 2001;58:570–92.
[16] Man H, Zhao N, Cui Z. Surface morphology of a laser surface nitride and etched Ti–6Al–4V alloy. Surf Coating Technol 2005;192:341–6.
[17] Gidley J, Openshaw S, Pring ET, Sale S, Mansell JP. Lysophosphatidic acid cooperates with 1α,25(OH)2D3 in stimulating human MG63 osteoblast maturation. Prostagl other Lipid Mediat 2006;80:46–61.
[18] Mansell JP, Farrar D, Jones S, Nowghani M. Cytoskeletal reorganisation, 1α,25-dihydroxy vitamin D3 and human MG63 osteoblast maturation. Mol Cell Endocrinol 2009;305:38–46.
[19] Mansell JP, Nowghani M, Pabbruwe M, Paterson IC, Smith AJ, Blom AW. Lysophosphatidic acid and calcitriol co-operate to promote human osteoblastogenesis: requirement of albumin-bound LPA. Prostagl other Lipid Mediat 2011;95:45–52.
[20] Mansell JP, Cooke M, Read M, Rudd H, Shiel AI, Wilkins K, et al. Chitinase 3-like 1 expression by human (MG63) osteoblasts in response to lysophosphatidic acid and 1,25-dihydroxyvitamin D3. Biochimie 2016;128-129:193–200.
[21] Lancaster S, Mansell JP. The role of lysophosphatidic acid on human osteoblast formation, maturation and the implications for bone health and disease. Clin Lipidol 2013;8:123–35.
[22] Paz Y. Self-assembled monolayers and titanium dioxide: from surface patterning to potential applications. Beilstein J Nanotechnol 2011;2:845–61.
[23] Queffélec C, Petit M, Janvier P, Knight DA, Bujoli B. Surface modification using phosphonic acids and esters. Chem Rev 2012;112:3777–807.
[24] Mansell JP, Brown J, Knapp JG, Faul CFJ, Blom AW. Lysophosphatidic acid-functionalised titanium as a superior surface for supporting human osteoblast (MG63) maturation. Eur Cell Mater 2012;23:348–61.
[25] Lancaster ST, Blackburn J, Blom A, Makishima M, Ishizawa M, Mansell JP. 24,25-Dihydroxyvitamin D3 cooperates with a stable, fluoromethylene LPA receptor agonist to secure human (MG63) osteoblast maturation. Steroids 2014;83:52–61.
[26] Ayre WN, Scott T, Hallam K, Blom AW, Denyer S, Bone HK, et al. Fluorophosphonate-functionalised titanium via a pre-adsorbed alkane phosphonic acid: a novel dual action surface finish for bone regenerative applications. J Mater Sci: Mater Med 2016;27:36.
[27] Neary G, Blom AW, Shiel AI, Wheway G, Mansell JP. Development and biological evaluation of fluorophosphonate-modified hydroxyapatite for orthopaedic applications. J Mater Sci Mater Med 2018;29:122.
[28] DeLory GE, King EJ. A sodium carbonate-bicarbonate buffer for alkaline phosphatases. Biochem J 1945;39:245.
[29] Payton OD, Picco L, Scott TB. High-speed atomic force microscopy for materials science. Int Mater Rev 2016;61:473–94.
[30] Cullen PL, Cox KM, Bin Subhan MK, Picco L, Payton OD, Buckley DJ, et al. Ionic solutions of two-dimensional materials. Nat Chem 2017;9:244–9.

[31] Mikheikin A, Olsen A, Leslie K, Russell-Pavier F, Yacoot A, Picco L, et al. DNA nanomapping using CRISPR-Cas9 as a programmable nanoparticle. Nat Commun 2017;8:1665.
[32] Puleo DA, Kissling RA, Sheu MS. A technique to immobilize bioactive proteins, including bone morphogenetic protein-4 (BMP-4), on titanium alloy. Biomaterials 2002;23:2079–87.
[33] Kashigawi K, Tsuji T, Shiba K. Directional BMP-2 for functionalization of titanium surfaces. Biomaterials 2009;30:1166–75.
[34] Roach P, Farrar D, Perry CC. Surface tailoring for controlled protein adsorption: effect of topography at the nanometer scale and chemistry. J Am Chem Soc 2006; 128:3939–45.
[35] Godoy-Gallardo M, Guillem-Marti J, Savilla P, Manero JM, Gil FJ, Rodriguez D. Anhydride-functional silane immobilized onto titanium surfaces induces osteoblast cell differentiation and reduces bacterial adhesion and biofilm formation. Mater Sci Eng C 2016;59:524–32.
[36] Ravanetti F, Gazza F, D'Arrigo D, Graiani G, Zamuner A, Zedda M, et al. Enhancement of peri-implant bone osteogenic activity induced by a peptidomimetic functionalization of titanium. Ann Anat 2018;218:165–74.
[37] Sano K, Shiba KA. Hexapeptide motif that electrostatically binds to the surface of titanium. J Am Chem Soc 2003;125:14234–5.
[38] Hayashi T, Sano K, Shiba K, Kumashiro Y, Iwahori K, Yamashita I, et al. Mechanism underlying specificity of proteins targeting inorganic materials. Nano Lett 2006;6: 515–9.
[39] Blackburn J, Mansell JP. The emerging role of lysophosphatidic acid (LPA) in skeletal biology. Bone 2012;50:756–62.
[40] Mansell JP, Barbour M, Moore C, Nowghani M, Pabbruwe M, Sjostrom T, et al. The synergistic effects of lysophosphatidic acid receptor agonists and calcitriol on MG63 maturation at titanium and hydroxyapatite surfaces. Biomaterials 2010;31: 199–206.
[41] Whyte MP. Physiological role of alkaline phosphatase explored in hypophosphatasia. Ann N Y Acad Sci 2010;1192:190–200.
[42] Mansell JP, Shiel AI, Harwood C, Stephens D. Alkaline phosphatase binds tenaciously to titanium; implications for biological surface evaluation following bone implant retrieval. Mater Sci Eng C Mater Biol Appl 2017;76:472–6.
[43] Yimsiri P, Mackley MR. Spin and dip coating of light-emitting polymer solutions: matching experiment with modelling. Chem Eng Sci 2006;61:3496–505.
[44] Fu L, Yu AM. Carbon nanotubes based thin films: fabrication, characterization and applications. Rev Adv Mater Sci 2014;36:40–61.
[45] Chaki SH, Mahato KS, Malek TJ, Deshpande MP. $CuAlS_2$ thin films - dip coating deposition and characterization. J Sci Adv Mater Devices 2017;2:215–24.
[46] Zhao SF, Jiang QH, Peel S, Wang XX, He FM. Effects of magnesium-substituted nanohydroxyapatite coating on implant osseointegration. Clin Oral Implants Res 2013;24(Suppl A100):34–41.
[47] Kopf BS, Schipanski A, Rottmar M, Berner S, Maniura-Weber K. Enhanced differentiation of human osteoblasts on Ti surfaces pre-treated with human whole blood. Acta Biomater 2015;19:180–90.
[48] Liu C, Dong JY, Yue LL, Liu SH, Wan Y, Liu H, et al. Rapamycin/sodium hyaluronate binding on nano-hydroxyapatite coated titanium surface improves MC3T3-E1 osteogenesis. PloS One 2017;12(2). e0171693.
[49] He R, Lu Y, Ren J, Wang Z, Huang J, Zhu L, et al. Decreased fibrous encapsulation and enhanced osseointegration in vitro by decorin-modified titanium surface. Colloids Surf B Biointerfaces 2017;155:17–24.
[50] Lai K, Xi Y, Miao X, Jiang Z, Wang Y, Wang H, et al. PTH coatings on titanium surfaces improved osteogenic integration by increasing expression levels of BMP-2/ Runx2/Osterix. RSC Adv 2017;7(89):56256–65.
[51] Yuan Z, Liu P, Liang Y, Bailong T, He Y, Hao Y, et al. Investigation of osteogenic responses of Fe-incorporated micro/nano-hierarchical structures on titanium surfaces. J Mater Chem B 2018;6(9):1359–72.
[52] Liu K, Zhang H, Lu M, Liu L, Yan Y, Chu Z, et al. Enhanced bioactive and osteogenic activities of titanium by modification with phytic acid and calcium hydroxide. Appl Surf Sci 2019;478:162–75.
[53] Zhao Q, Yi L, Jiang L, Ma Y, Lin H, Dong J. Surface functionalization of titanium with zinc/strontium-doped titanium dioxide microporous coating via microarc oxidation. Nanomedicine 2018;16:149–61.
[54] Pierre CG, Bertrand G, Rey C, Benhamou O, Combes C. Calcium phosphate coatings elaborated by the soaking process on titanium dental implants: surface preparation, processing and physical-chemical characterization. Dent Mater 2019;35(2):e25–35.
[55] Huang TB, Li YZ, Yu K, Yu Z, Wang Y, Jiang ZW, et al. Effect of the Wnt signal-RANKL/OPG axis on the enhanced osteogenic integration of a lithium incorporated surface. Biomater Sci 2019;7(3):1101–16.